Isomeric and ground-state properties of $^{171}_{78}$Pt, $^{167}_{76}$Os, and $^{163}_{74}$W

C. Scholey,[1,*] K. Andgren,[2] L. Bianco,[3,†] B. Cederwall,[2] I. G. Darby,[1,3,‡] S. Eeckhaudt,[1] S. Ertürk,[4] M. B. Gomez Hornillos,[5,§] T. Grahn,[1,‖] P. T. Greenlees,[1] B. Hadinia,[2,¶] E. Ideguchi,[6] P. Jones,[1] D. T. Joss,[3] R. Julin,[1] S. Juutinen,[1] S. Ketelhut,[1] M. Leino,[1] A.-P. Leppänen,[1,**] P. Nieminen,[1] M. Niikura,[6] M. Nyman,[1] D. O'Donnell,[5] R. D. Page,[3] J. Pakarinen,[1,††] P. Rahkila,[1] J. Sarén,[1] M. Sandzelius,[1,2] J. Simpson,[5] J. Sorri,[1] J. Thomson,[3] J. Uusitalo,[1] and M. Venhart[1,7,‡]

[1]*University of Jyväskylä, Department of Physics, PO Box 35, FI-40014 Jyväskylä, Finland*

[2]*Royal Institute of Technology, S-106 91 Stockholm, Sweden*

[3]*Oliver Lodge Laboratory, University of Liverpool, Liverpool, L69 7ZE, United Kingdom*

[4]*Department of Physics, Nigde University, 51200 Nigde, Turkey*

[5]*STFC, Daresbury Laboratory, Daresbury, Warrington WA4 4AD, United Kingdom*

[6]*Center for Nuclear Study, University of Tokyo, Wako, Saitama 351-0198, Japan*

[7]*Department of Nuclear Physics and Biophysics, Comenius University, 84248 Bratislava, Slovakia*

(Received 29 October 2009; published 15 January 2010)

Decay paths, half-lives, and excitation energies of the $i_{13/2}$ bandheads of the neutron-deficient nuclei ^{171}Pt, ^{167}Os, and ^{163}W have been established for the first time. Gamma-ray transitions, X-rays, and internal conversion electrons have been observed, allowing internal-conversion coefficients to be measured and $B(M2)$ reduced transition probabilities to be extracted. These results elucidate the low-lying single-quasiparticle structures and give the energy level spacings between the $\nu f_{7/2}$, $\nu h_{9/2}$, and $\nu i_{13/2}$ quasineutron states for all three nuclei. Moreover, ground-state spin assignments have been made for the first time, along with the measurement of the α-decay branching ratio for ^{171}Pt. The decay paths of the $i_{13/2}$ bandheads were followed by favored α decays, indicating that all three nuclei have the same $I^{\pi} = 7/2^{-}$ ground state.

DOI: 10.1103/PhysRevC.81.014306 PACS number(s): 27.70.+q, 21.10.Tg, 23.20.Lv, 23.20.Nx

I. INTRODUCTION

Unique-parity shell-model intruder orbitals have a profound effect on electromagnetic transitions in and the decay properties of nuclei. The large spin and small energy differences between these intruder states and other states near the Fermi surface, result in excited states based on these orbitals often being isomeric. In the region of very neutron-deficient nuclei below the $Z = 82$ shell gap, both the $\pi h_{11/2}$ and $\nu i_{13/2}$ intruder orbitals are present around the Fermi surface. The Hg-Pt-Os-W nuclei in this region are in the vicinity of both the N and $Z = 82$ closed shells. These facts give rise to a region of transitional nuclei with small deformations, exhibiting both single-particle and rotational characteristics.

In neutron-deficient odd-A Pb nuclei two α-decaying states have been observed for $A < 189$, the $3/2^{-}$ ground state, and an excited $13/2^{+}$ state [1–3], while in the light odd-A Hg-Pt-Os-W nuclei only one α-decaying state has been observed [4,5]. Unlike odd-A Pb nuclei, in these latter nuclei the lowest-lying $13/2^{+}$ state does not decay via charged particle emission, leading to the assumption that there must be a decay path to the ground state. For ^{179}Hg [3], ^{177}Hg [6], and ^{175}Hg [7] this decay path has been observed. In these cases the $13/2^{+}$ state was observed to be isomeric, depopulated via an $M2$ γ-ray transition to a $9/2^{-}$ state, then proceeding to the $7/2^{-}$ ground state via an $M1$ γ-ray transition. The decay of the $13/2^{+}$ state in ^{179}Hg was identified following the α decay of ^{183}Pb [3], while ^{177}Hg [6] and ^{175}Hg [7] were investigated using a combination of recoil-decay tagging (RDT) [8,9] and recoil-isomer tagging (RIT) [10,11]. The ground-state spin and parity of these nuclei were assigned based on these measurements. In contrast, the decay paths from analogous states in many of the neutron-deficient odd-A Pt, Os, and W nuclei have not been determined, yet yrast structures based on the $\nu i_{13/2}$ configuration have been observed. The assignment was made on the basis of energy level systematics across isotopic and isotonic chains, but in many cases it has not been possible to assign the ground-state spin and parity or determine the excitation energies of the $13/2^{+}$ states relative to the ground state. This renders it impossible to determine the relative positions of states based on specific neutron orbitals in these odd-N nuclei. Examples of nuclei that have 'floating' $13/2^{+}$ bandheads are ^{171}Pt, ^{167}Os, and ^{163}W, which are the focus of this work. In the case of ^{171}Pt and ^{167}Os, prior to experiments reported on in this work, RDT studies were performed and excited states built on a $\nu i_{13/2}$ state were observed [12–15]. Excited states were assigned to ^{163}W on the basis of X-ray

*cs@phys.jyu.fi

†Present address: Department of Physics, University of Guelph, Guelph, Ontario N1G2W1, Canada.

‡Present address: Instituut voor Kern- en Stralingsfysica, University of Leuven, Celestijnenlaan 200 D, B-3001 Leuven, Belgium.

§Present address: Universidad Politécnica Catalunã, E-08021 Barcelona, Spain.

‖Present address: Oliver Lodge Laboratory, University of Liverpool, Liverpool L69 7ZE, UK.

¶Present address: University of the West of Scotland, High street, PA1 2BE Paisley, UK.

**Present address: STUK, Rovaniemi, Finland.

††Present address: ISOLDE, CERN CH-1211 Geneva 23, Switzerland.

coincidences with γ rays [16,17]. In all cases, states below the $13/2^+$ state were not observed. Despite the lack of firm spin and parity assignments for the ground states of these nuclei, various predictions have been made. Audi *et al.* [18] estimated from systematic trends of neighboring nuclei with the same Z or N, that the spins and parities of the ground states of ^{171}Pt, ^{167}Os, and ^{163}W are all $3/2^-$; however, Möller, Nix and Kratz [19], using a mean field approach, predicted spins and parities of $3/2^-$, $5/2^+$, and $1/2^-$, respectively.

This paper reports on the decay paths from the $13/2^+$ state in the α-decay chain nuclei, ^{171}Pt, ^{167}Os, and ^{163}W to the ground state, for the first time. Conversion electron and γ-ray measurements have fixed the excitation energies of the $13/2^+$ states and the half-lives of these states have been measured, establishing that they are isomeric. The multipolarities of transitions in the decay paths to the ground states have been determined providing information on the spins and parities of these states for the first time. Also, α-decay hindrance factors have been extracted verifying the isomer-decay spectroscopy result, that all three nuclei have the same spin and parity ground state.

II. EXPERIMENTAL DETAILS

The experiments were performed at the Accelerator Laboratory of the University of Jyväskylä. Heavy ion beams were accelerated by the K-130 cyclotron and impinged onto thin self-supported isotopically enriched metallic targets, resulting primarily in fusion-evaporation reactions. For all reactions a carbon "reset" foil of $\approx$50 μg/cm^2 was placed directly downstream of the target. The tungsten, osmium, and platinum nuclei of interest were produced using different reactions, the details of which are summarized in Table I. For all cross section estimates the DSSDs coverage was taken to be 75%; 45% of α particles are expected to have escaped the DSSDs without depositing their full energy and the gas-filled separator RITU's [20] transmission was taken to be 35% for $2pn$ exit channels and 20% for $\alpha 2pn$ exit channels.

Prompt γ rays from the fusion-evaporation reactions were detected by the JUROGAM γ-ray spectrometer [21]. JUROGAM comprises 43 escape-suppressed EUROGAM phase-I [22] and GASP [23] type HPGe detectors, positioned in six rings around the target position, giving a total photopeak efficiency of $\sim$4.3% at 1.3 MeV.

Recoiling fusion-evaporation residues recoils were separated in-flight from primary beam and beam-like particles by the gas-filled separator RITU [20]. At the focal plane of RITU the recoils pass through a multi-wire proportional counter (MWPC) and are implanted into one of the two adjacent double-sided silicon strip detectors (DSSDs), of the GREAT spectrometer [24]. A time-of-flight (TOF) was measured between the DSSDs and the MWPC. Recoiling nuclei were initially identified from a two-dimensional plot of the energy loss signal in the MWPC versus TOF. The implantation DSSDs were 300 μm thick with dimensions of 60 $\times$ 40 mm and a strip pitch of 1 mm giving a total of 4800 pixels. The high pixelation allowed accurate temporal and spatial correlations between implanted recoils and all subsequent α decays. Surrounding the DSSDs, directly up stream with respect to the beam direction, were two rings of Si PIN-diodes of 500 μm thickness and dimensions of 28 $\times$ 28 mm to detect conversion electrons and α particles which escape from the DSSDs.

Gamma-ray detection at the RITU focal plane was provided by a planar Ge detector, placed directly behind the DSSDs, within the vacuum chamber and a clover Ge detector, placed directly above the focal plane chamber. The combination of these two Ge detectors was calculated to give a total photopeak efficiency of $\sim$2% at 1.3 MeV and $\sim$20% at 100 keV [25]. In addition, two large volume clover detectors were added to the focal plane detection system, one on either side of the chamber for reaction 1 and the latter half of the experiment using reaction 5, giving a total photopeak efficiency of $\sim$4.6% and $\sim$25% at 1.3 MeV and 100 keV, respectively [25]. These Ge detectors along with the JUROGAM array gave the opportunity to simultaneously detect γ rays with a high efficiency at both the target position and focal plane of the RITU separator. They allowed the RIT technique to be exploited, which is particularly useful if the nuclei of interest do not have a charged-particle decay mode suitable for RDT. Combining decay spectroscopy, RDT and RIT for both γ rays and conversion electrons allowed near 'complete' spectroscopy to be performed, hence filling in missing links between structures which feed or bypass an isomeric state. Once γ rays at the focal plane were identified the half-life of the state was obtained by measuring the time difference between a recoil implant in the DSSDs and subsequent γ rays. For the more highly converted transitions, the time between the recoils in the DSSDs and conversion electrons in the PIN diodes also yields the half-life of the state, verifying the results obtained from the γ-ray data.

These data were collected through the triggerless total data readout (TDR) data acquisition system [26]. All events were

TABLE I. Fusion-evaporation reaction details for populating the nuclei of interest. The isotopic enrichment for the ^{92}Mo, ^{96}Ru, and ^{106}Cd targets were 97.3%, 96%, and 96.47%, respectively. The number in the left-most column is used in the text in reference to these reactions.

Reaction number	Nucleus	Beam			Target		Exit Channel	Irradiation time (hrs)	Implantation Rates (Hz)	cross-section
		Isotope	Energy (MeV)	I (pnA)	Isotope	Thickness (μg/cm^2)				
1	^{163}W	^{60}Ni^{12+}	270	4	^{106}Cd	1100	$2pn$	121	1500	$\sim$4 mb
2	^{163}W	^{78}Kr^{15+}	380	5	^{92}Mo	500	$\alpha 2pn$	160	400	$\sim$0.7 mb
3	^{167}Os	^{78}Kr^{15+}	365	5	^{92}Mo	500	$2pn$	67	1000	$\sim$2 mb
4	^{167}Os	^{78}Kr^{15+}	357	5	^{92}Mo	500	$2pn$	23	1000	$\sim$2 mb
5	^{171}Pt	^{78}Kr^{15+}	348	10	^{96}Ru	500	$2pn$	140	60	$\sim$85 μb

read out individually, time stamped with a precision of 10 ns by a 100 MHz metronome and merged into a single stream of time-stamped events. These data were prefiltered before being written to disk. In this case, all focal plane events and any event which occurred 5 μs ($\sim$10 times the flight time of RITU) before the focal plane events were written to disk. These data were analysed on- and off-line with the GRAIN analysis package [27]. A series of two-dimensional matrices were constructed and analyzed off-line using GRAIN [27] and the UPAK [28] analysis package.

III. RESULTS

Alpha decay branching ratios for ^{171}Pt, ^{167}Os, and ^{163}W have been measured. Due to the low background registered in the focal plane Ge detectors, branching ratios for the α decay of these nuclei was determined from the ratio of recoil-gated delayed γ rays to α-tagged delayed γ rays. In these measurements, 55(5)% of the α decays were observed in the full energy α peak and a correction was made to the number of decays measured to account for the search time of the α correlations. All other factors cancel apart from the branching ratio. Branching ratios of 83(3)%, 51(5)%, and 15(2)% were measured for ^{171}Pt, ^{167}Os, and ^{163}W, respectively. The nuclei of ^{163}W and ^{167}Os were produced through the α-decay chain of ^{171}Pt, therefore the α-decay branching ratios were also obtained from recoil-α-α-α correlations from the reaction 5 data set, thus verifying the results obtained from delayed γ-ray coincidences. The results for ^{167}Os and ^{163}W are consistent with the literature values [4], while the α-decay branching ratio for ^{171}Pt is measured for the first time. The hindrance factors for the α decay of ^{171}Pt, ^{167}Os, and ^{163}W were calculated to be 1.1(1), 1.1(1), and 0.8(1), respectively, using $\mathrm{HF} = t_{1/2}^{\mathrm{expt}}/t_{1/2}^{\mathrm{ras}}$, where $t_{1/2}^{\mathrm{expt}}$ is the experimental α-decay partial half-life from this work (reported in the following subsections) and $t_{1/2}^{\mathrm{ras}}$ is the α-decay partial half-life calculated using the Rasmussen method [29]. These values are consistent with $\Delta l = 0$ transitions, indicating that there is no change in spin or parity between these α-decaying states, assuming they are ground-state–to–ground-state decays. These values are also consistent with $\Delta l = 1$ transitions. If this was the case then fine-structure α decay may occur. A search for α-decay fine structure was undertaken, but none was observed. Therefore we conclude that all three α decays are $\Delta l = 0$, hence all α-decaying states have the same spin and parity. The ground state of ^{159}Hf, the α decay daughter of ^{163}W, is reported to have a ground state spin and parity of $I^{\pi} = 7/2^{-}$ [30] as do the subsequent nuclei in the α-decay chain [31,32]. The $I^{\pi} = 7/2^{-}$ assignment of Ref. [30] is ambiguous and therefore cannot be solely used for assigning the spin and parity of the heavier α-decay chain partners. However, arguments supporting the assignment of $I^{\pi} = 7/2^{-}$ to the ground states of ^{171}Pt, ^{167}Os, and ^{163}W will be presented in the following subsections.

A. $^{163}_{74}W_{89}$

Nuclei of ^{163}W were produced directly in reactions 1 and 2, detailed in Table I. In reactions 1 and 2 a total of 4.5×10^6 and 4.8×10^5 recoil-α (^{163}W) correlated nuclei, respectively, were collected within a total search time of 3 s. Correlated α-decay energy spectra from reactions 1 and 2 are shown in Figs. 1(a) and 1(b), respectively.

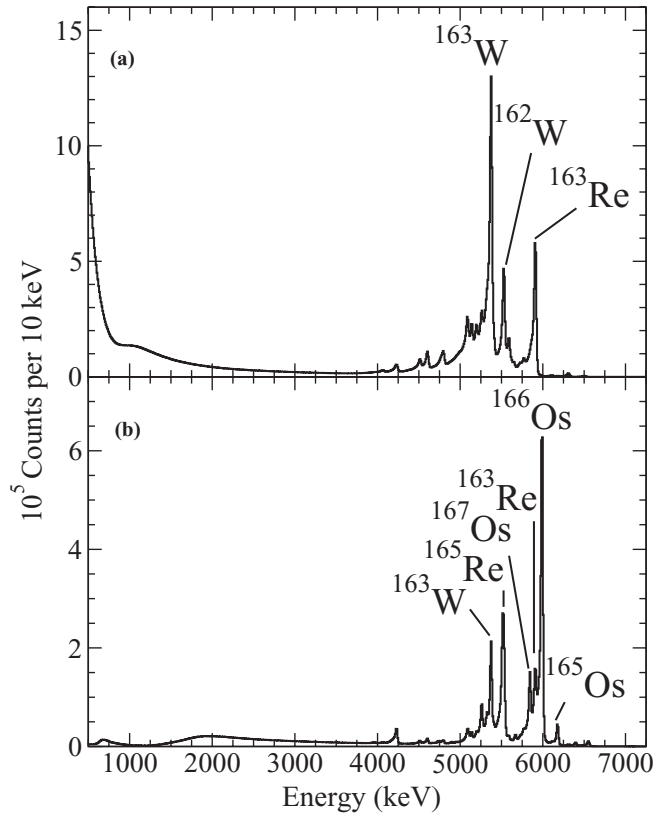

FIG. 1. Spectra of α-decay energies correlated to a recoil implant within the same pixel of the DSSDs at the focal plane of RITU, within a maximum correlation time of 3 s are shown in (a) and (b) for reactions 1 and 2, respectively.

The α-decay half-life was determined from data collected from reaction 5. This reaction was favored for the half-life measurement since the lower recoil implantation rate in the DSSDs reduced the possibility of false recoil-α correlations, due to the relatively long α-decay half-life of ^{163}W. The decay curve featured in Fig. 2 shows the time differences between the detection of a characteristic α decay of ^{163}W and its mother decay of ^{167}Os. The α decay of ^{167}Os, was already correlated to its mother α decay ^{171}Pt and the initial implanted recoil in the DSSDs. Thus, the α-decay half-life from the ground state of ^{163}W was measured to be $t_{1/2} = 2.6(1)$ s, which is consistent with previous measurements of 3.0(1.3) [4], 2.8(2) [34], and 2.5(3) [35]. The ^{163}W α-particle energy of 5383(6) keV [4] was used as one of the internal α-decay calibration points, hence no improvement to this value was obtained from this work.

In order to search for γ-ray emissions from long-lived states in ^{163}W, the characteristic α decays have been utilized as a selective tag. Due to the relatively long α-decay half-life and low branching ratio, the α decay of ^{163}W was only used as an initial tag, in order to determine the origin of the γ rays detected in the focal plane Ge detectors. Figures 3(a) and 3(b) show the spectra obtained from the clover and planar

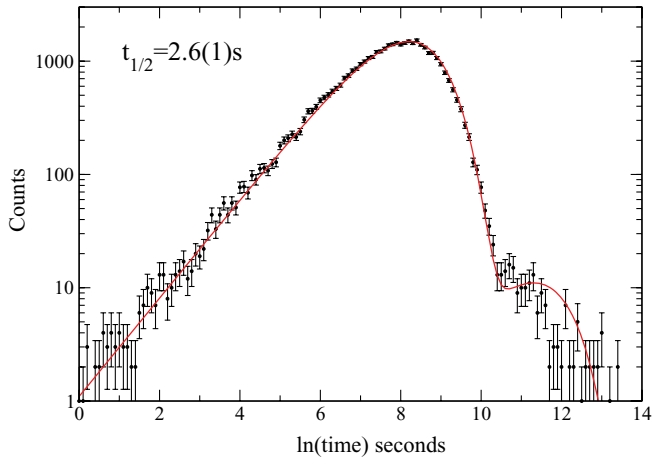

FIG. 2. (Color online) The decay curve of the α decay of ^{163}W, taken as the time difference between the α decays of ^{167}Os and ^{163}W subsequent to the α decay of ^{171}Pt in reaction 5. The maximum search time between a recoil and ^{171}Pt α decays, ^{171}Pt α decays, and ^{167}Os α decays were 150 ms and 3 s, respectively. The fit to the data was produced using Eq. (8) in Ref. [33] and is shown in by the solid/red line.

detectors[1] within 1 μs of recoil implants in the DSSDs from reactions 1 and 2, respectively. Figures 3(c) and 3(d) show

[1]The counts at very low energy in these spectra and in all focal plane γ-ray spectra shown in this paper are a consequence of a combination of low-energy thresholds, low-energy γ rays, and X-rays and a nonlinear ADC response in the lower channels. The photopeaks in the planar Ge detector spectra have low-energy tails due to incomplete charge collection.

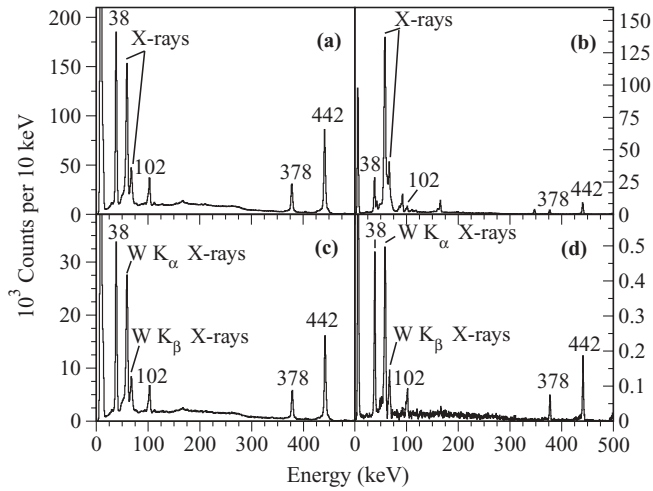

FIG. 3. Recoil-gated and ^{163}W α-tagged γ-ray spectra taken from the clover and planar Ge detectors at the focal plane of RITU. In all cases, γ rays were collected up to 1 μs after a recoil implant in the DSSDs. (a) A spectrum of recoil-gated γ-rays from reaction 1. (b) A recoil-gated γ-ray spectrum from reaction 2. (c) and (d) are the same as (a) and (b), respectively, with the additional requirement that the recoil implantation is followed by an α decay of ^{163}W in the same DSSDs pixel within 3 s of the recoil.

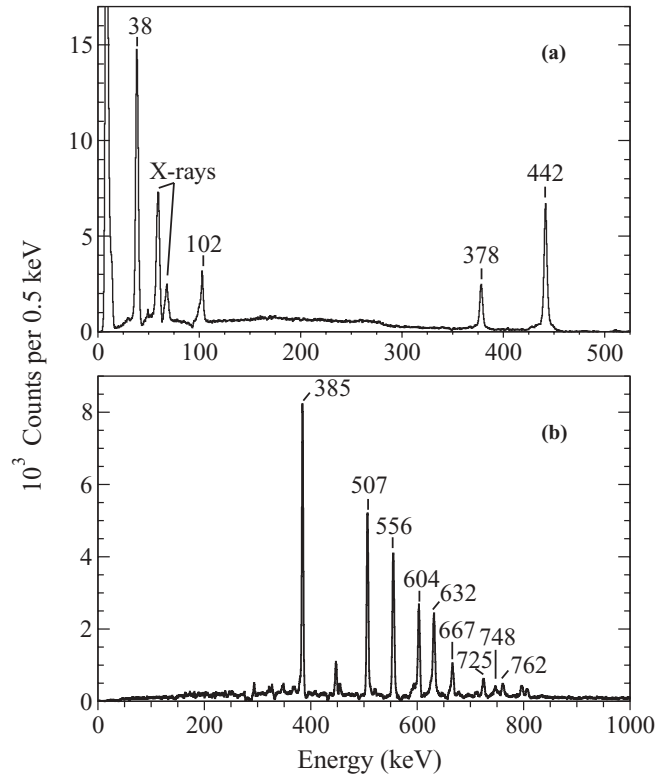

FIG. 4. (a) A summed energy spectrum of γ rays detected in the GREAT planar and clover detectors within 1 μs of a recoil implantation in the DSSDs and correlated with the yrast band γ-ray transitions labeled in (b), of ^{163}W detected in JUROGAM up to 2 μs before a recoil implant. (b) Spectrum showing γ rays detected in JUROGAM in delayed coincidence with the 38 keV, 102 keV, 378 keV, and 442 keV γ rays detected in the GREAT planar and clover detectors. The γ rays form the yrast band of ^{163}W. Each spectrum reflects the combined data from reactions 1 and 2.

the effect of providing an additional requirement, that the recoil implantation is followed by a ^{163}W α decay in the same pixel within 3 s. The latter two spectra unambiguously assign the γ rays with energies of, 38.4(7), 102.1(7), 378.3(6), and 441.7(7) keV to ^{163}W.

The first observation of the excited states in ^{163}W was made by Dracoulis *et al.* who observed a collective band assigned to be based upon a $\nu i_{13/2}$ state [16,17]. In order to ascertain if the previously observed yrast band feeds the isomeric state observed in the present work, searches for prompt-delayed γ-ray correlations (RIT) were performed. Figure 4(a) shows γ rays detected at the focal plane up to 1 μs after a recoil implantation, that are correlated with γ-ray transitions in the yrast band of ^{163}W detected in the JUROGAM array. The 38 keV, 102 keV, 378 keV, and 442 keV γ rays and characteristic W K_α and K_β X-rays can be clearly seen in the resulting spectrum. The converse spectrum using the γ-ray transitions detected at the focal plane as a tag to identify states above the isomer is perhaps more striking. Figure 4(b) shows that the yrast band of ^{163}W is selected unambiguously with RIT.

In addition to γ-ray transitions, a search for conversion electrons in the PIN diodes was performed. Figure 5 shows

TABLE II. Properties of the transitions in the decay path of the $i_{13/2}$ isomeric state in ^{163}W, ^{167}Os, and ^{171}Pt. α_K^{theory} and $\alpha_K/\alpha_{LM}^{\text{theory}}$ were taken from Ref. [36].

Nuclei	E_γ (keV)	I_γ[a]	α_K^{expt}	α_K^{theory}	$\alpha_K/\alpha_{LM}^{\text{expt}}$	$\alpha_K/\alpha_{LM}^{\text{theory}}$	σL	I_{tot}	E_i	$I_i^\pi \rightarrow I_f^\pi$
^{163}W										
	38.4(7)	52(7)	–	13.8($M1$), 0.99($E1$)	–	–	$E1$	100(20)	480.1	$13/2^+ \rightarrow 11/2^-$
	102.1(7)	7(1)	4.1(4)	4.49($M1$), 3.75($E2$)	–	–	$M1$	38(6)	102.1	$9/2^- \rightarrow 7/2^-$
	378.3(6)	30(4)	0.46(9)	0.12($M1$), 0.41($M2$)	3.7(7)	5.3($M1$), 4.1($M2$)	$M2$	40(10)	480.4	$13/2^+ \rightarrow 9/2^-$
	441.7(7)	100(14)	0.022(3)	0.08($M1$), 0.03($E2$)	3.3(7)	6.3($M1$), 3.1($E2$)	$E2$	99(30)	441.7	$11/2^- \rightarrow 7/2^-$
^{167}Os										
	86.7(8)	16(2)	7.0(1)	6.9($M1$), 0.91($E2$)	–	–	$M1$	94(18)	86.7	$9/2^- \rightarrow 7/2^-$
	347.6(8)	100(14)	0.5(1)	0.49($M2$), 0.11($E3$)	–	–	$M2$	100(20)	434.3	$13/2^+ \rightarrow 9/2^-$
^{171}Pt										
	89.5(7)	19(3)	7.5(10)	7.52($M1$), 0.77($E2$)	–	–	$M1$	99(15)	89.5	$9/2^- \rightarrow 7/2^-$
	323.1(6)	100(14)	0.65(12)	0.72($M2$), 0.14($E3$)	3.5(5)	3.6($M2$), 0.64($E3$)	$M2$	100(21)	412.6	$13/2^+ \rightarrow 9/2^-$

[a] I_γ is given relative to the strongest γ-ray photopeaks in the α-tagged focal-plane γ-ray spectrum for a given nucleus.

a conversion electron spectrum from the PIN diodes within 1 μs of a recoil implant in the DSSDs. Peaks corresponding to the K, L, and M conversion electrons from the 378 keV and 442 keV transitions are clearly visible.

Two-dimensional matrices of delayed γ rays and conversion electrons were constructed. This allowed the ordering of the excited states in the decay path from the isomer by means of γ-γ and CE-γ ray coincidences, sample spectra of which are shown in Fig. 6.

Figure 6 provides evidence for two parallel decay paths from the isomeric state. One branch is comprised of transitions with energies of 38.4(7) keV and 441.7(7) keV and the other 102.1(7) keV and 378.3(6) keV. If the observed de-excitation constitutes the decay path to the ground state, these coincidences assign an excitation energy of 480.3(3) keV to the isomeric state. Internal K-shell conversion coefficients (α_K) were extracted from the ratio of K X-rays to γ rays. The 38 keV transition energy is below the K-shell electron-binding energy, therefore no K-shell internal conversion occurs and the

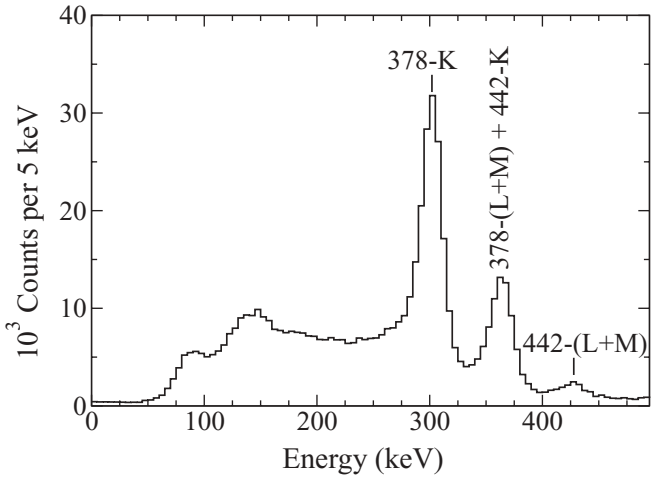

FIG. 5. Conversion electron spectrum from the PIN diodes taken within 1 μs of recoil implant in the DSSDs from reaction 1. The labeled peaks are assigned to ^{163}W.

L-shell X-ray energies are below the energy threshold set on the detectors, hence could not be measured. The α_K values for the 102 keV, 378 keV, and 442 keV transitions were measured to be 4.1(4), 0.46(9), and 0.022(3), respectively, and are consistent with multipolarities of $M1$, $M2$, and $E2$, respectively. In addition, the α_K/α_{LM} ratios[2] of conversion electrons were measured to be 3.7(7)and 3.3(7) for the 378 keV and 442 keV transitions, respectively. These values are consistent with the theoretical α_K/α_{LM} values of 4.1 and 3.1 [36], for a 378 keV $M2$ transition and a 442 keV $E2$ transition, respectively. The analysis of the α_K/α_{LM} ratio required coincidences between γ rays and conversion electrons due the transition energy overlap of the 378-L and 442-K conversion electron energies. These coincidences are shown in the inset of Fig. 6(a) and 6(b). The internal-conversion electron results are summarized in Table II.

The decay curves for all delayed transitions were extracted from the time between a recoil implant and the γ-ray events in the clover or planar detectors. The half-life of the isomeric state was measured to be $t_{1/2} = 154(3)$ ns, by taking an average of all four γ-ray half-lives. Sample half-life decay curves are shown as insets in Figs. 6(c) and 6(d), for the 378 keV and 442 keV transitions.

Weisskopf single-particle estimates for a 102 keV $M1$, a 378 keV $M2$, and a 442 keV $E2$ transitions are 2.96 ps, 137 ns, and 624 ps, respectively. Taking into account the conversion coefficients from Table II, they suggest that the 378 keV $M2$ transition directly depopulates the isomeric state and that the 442 keV transition is too fast to be the parallel transition. This only leaves the 38 keV transition to be parallel to the 378 keV transition, as the 102 keV and 378 keV transitions are in coincidence. Efficiency and conversion corrected intensities, $I_{\text{tot}} = I_\gamma(1 + \alpha_{\text{tot}})$, were calculated and are tabulated in Table II. The intensity balance only fits if the 38 keV transition is an $E1$ transition with an $\alpha_{\text{tot}} = 1$. Even though a 38 keV $E1$ transition's half-life estimate is

[2] The L and M conversion electron energies could not be resolved, hence α_K/α_{LM} ratios were measured.

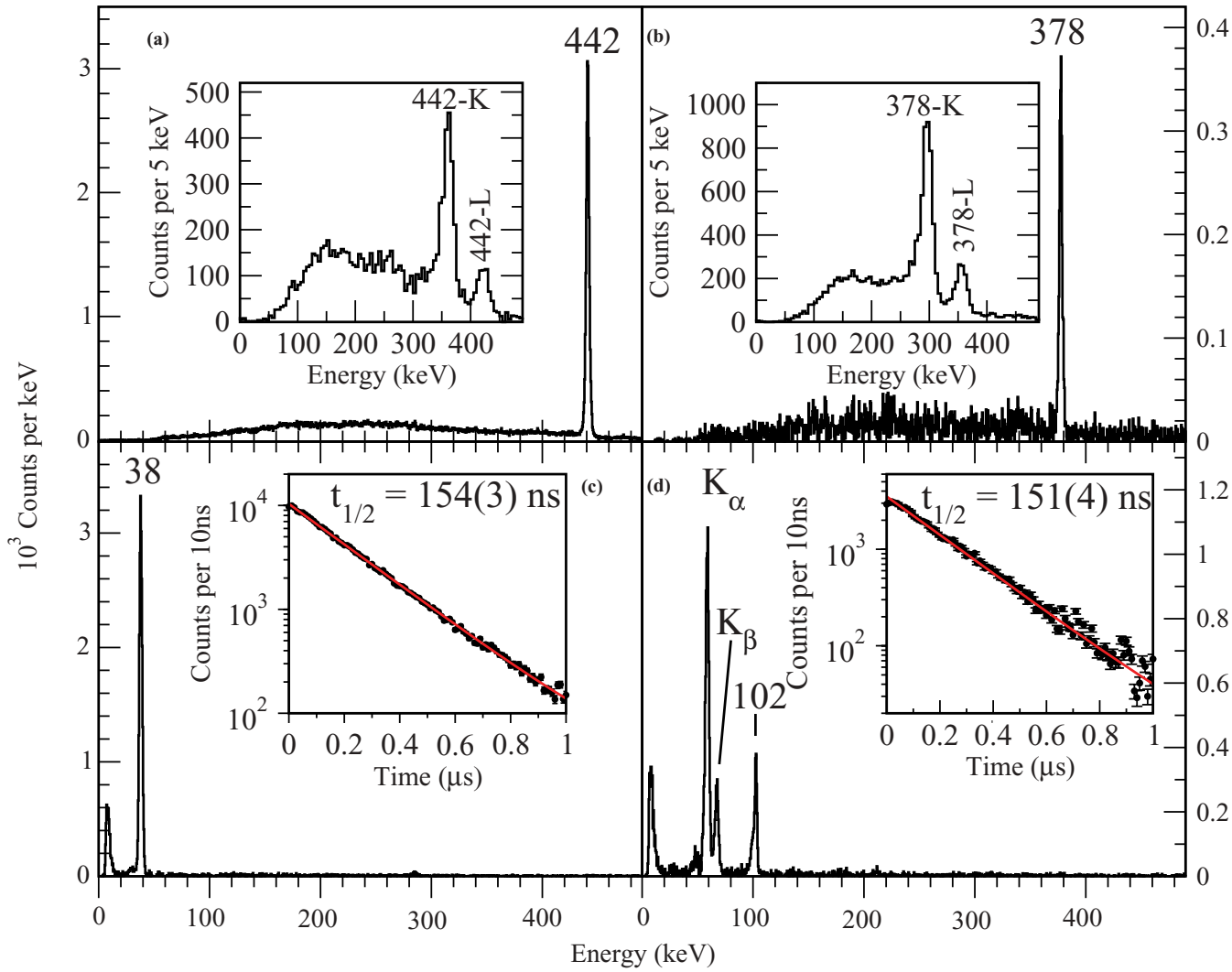

FIG. 6. (Color online) Spectra of transitions associated with ^{163}W. (a) Spectrum showing γ rays detected in the clover detectors in coincidence with 38 keV γ rays detected in the planar detector. Inset shows conversion electrons measured in the PIN-diodes in coincidence with 38 keV γ rays detected in the planar detector. (b) Same as (a), but for the 102 keV transition. (c) Spectrum showing γ rays detected in the planar in coincidence with 442 keV γ rays detected in the clover detector. Inset shows the decay curve generated by the time difference between a recoil implant in the DSSDs and a 442 keV γ ray in the clover or planar detectors. The solid line is an exponential fit to these data. (d) Spectrum showing γ rays detected in the planar detector in coincidence with 378 keV γ rays detected in the clover detector. The inset shows the decay curve of 378 keV γ rays from the time difference between a recoil in the DSSDs and a γ ray in either the clover or planar detectors. An exponential fit to the data is shown by the solid/red line.

4.0 ps, it is widely accepted that $E1$ transitions are severely hindered (typically by 10^5 [37]). Interestingly, the reduced transition probability $B(E1) = \frac{6.76\times10^6}{E^3 A^{\frac{2}{3}} t_{1/2}(1+\alpha_{\rm tot})/br\%}$ W.u. for the 38 keV transition is $9.5(2) \times 10^{-6}$ W.u., which is a hindrance of approximately 10^5. Higher multipoles produce half-lives an order of magnitude or more greater than the measured half-life of 154(3) ns, therefore they would not compete with the 378 keV $M2$ transition.

In conclusion, the only scenario that accommodates all these factors is if the 38 keV $E1$ and the 378 keV $M2$ transitions depopulate the isomeric state. It has been shown that the isomeric state is the $I^\pi = 13/2^+$ bandhead, therefore the 38 keV and 378 keV transitions feed states with $I^\pi = 11/2^-$ and $I^\pi = 9/2^-$, respectively. The decay from the $11/2^-$ state is via the 442 keV $E2$ transition, hence it feeds the $I^\pi = 7/2^-$ state, while the $I^\pi = 9/2^-$ state decays via a 102 keV $M1$ transition also to the $I^\pi = 7/2^-$. Any other combination would result in one branch being far faster than the other, hence it would be the dominant path. The branching ratios for the 378 keV and 38 keV decay paths were measured to be 29% and 71%, respectively. These findings are summarized in the partial level scheme of ^{163}W shown in Fig. 7. As there is no evidence for any other transitions below the $I^\pi = 7/2^-$ state, we conclude that it is the ground state. The result is consistent with the α-decay study presented earlier in this article. This

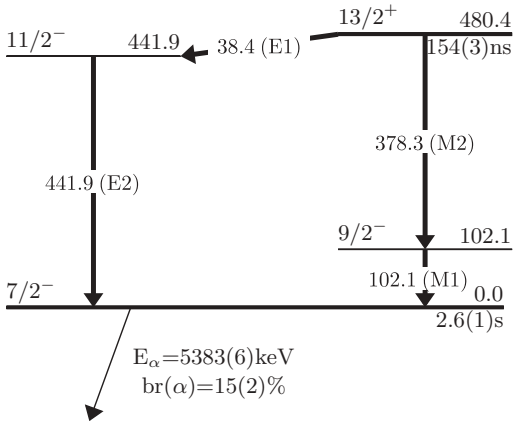

FIG. 7. A partial level scheme of ^{163}W showing the decay path from the $13/2^+$ isomeric state and the ground-state α-decay information. The α-decay energy is taken from Ref. [4].

firm assignment of $I^\pi = 7/2^-$ for the ground state of ^{163}W also establishes that the ground states of ^{167}Os and ^{171}Pt are $I^\pi = 7/2^-$ through the α-decay hindrance factors.

B. $^{167}_{76}$Os$_{91}$

Nuclei of ^{167}Os were produced using reactions 3 and 4, as shown in Table I. During reaction 3 the planar Ge detector was placed outside the focal plane chamber, directly behind the DSSDs and the clover detector was not present at all. During reaction 4 the planar detector was inside the focal plane chamber 8 mm behind the DSSDs and the clover detector was present. The PIN-diodes had a gain range of ≈8 MeV in order to detect escaping α particles from the DSSDs, therefore no conversion electron information was obtained. The number of recoil-(^{167}Os)α correlations produced in reactions 3 and 4 was 5.5×10^6. The ^{167}Os α-particle energy of 5853(5) keV [4] was used as one of the calibration points and is shown in Fig. 8(a) along with all other α decays correlated within 3 s of a recoil implanted in the DSSDs within the same pixel. In reaction 5 ^{167}Os was produced as the daughter decay of ^{171}Pt and from these data the α-decay half-life was measured to be $t_{1/2} = 839(5)$ ms, as is shown in Fig. 8(b). This result is consistent with previous measurements [4,38,39], but with improved precision. A total of 6.6×10^5 delayed γ rays were correlated with the α decay of ^{167}Os within 3 μs of a recoil implant in the DSSDs and are shown in Fig. 9(a). Two γ-ray photopeaks of energy 86.7(8) keV and 347.6(8) keV are clearly seen in addition to Os K_α and K_β X-rays. A γ-γ coincidence matrix between events in the clover and planar Ge detectors was constructed. Typical gated spectra from this matrix are shown in Figs. 9(b) and 9(c) and confirm that these two γ-ray transitions are in coincidence.

K-shell internal conversion coefficients were extracted from the γ-ray coincidence data, by measuring the ratio of K X-rays to γ rays. The measured α_K for the 87 keV and 348 keV transitions were 7.0(1) and 0.5(1), respectively. These values are consistent with theoretical values of $\alpha_K = 6.9$ for an 87 keV $M1$ transition and $\alpha_K = 0.49$ for a 348 keV $M2$ transition [36]. Values for any other multipolarities are more than order of magnitude away from the experimental α_K values. As the 87 keV and 348 keV transitions are in coincidence and no side-feeding is observed, their total intensities should be equal. The efficiency corrected intensity $I_{\text{tot}} = I_\gamma(1 + \alpha_{\text{tot}})$ was calculated using the transition multipolarities of $M1$ and $M2$ gained from the α_K measurements for the 87 keV and 348 keV, respectively. The results are shown in Table II and confirm that the intensities for an 87 keV $M1$ and an 348 keV $M2$ transition are equal.

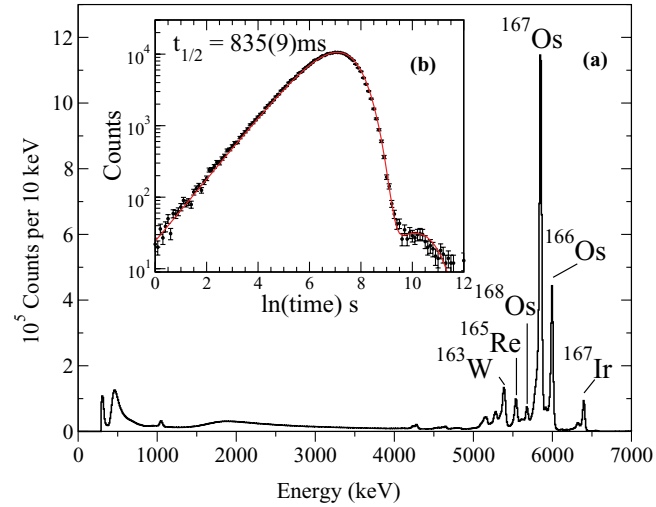

FIG. 8. (Color online) (a) An α-decay spectrum correlated within 3 s of a recoil is shown in (a), taken from reactions 3 and 4. (b) shows the decay curve of ^{167}Os correlated within 3 s of a ^{171}Pt parent decay, which is correlated to a recoil, using a maximum search time of 150 ms. These data were collected during experiment 5. The fit to the data was produced using Eq. (8) in Ref. [33] and is shown in by the solid/red line.

The half-life of the isomeric state was measured to be $t_{1/2} = 700(10)$ ns and example decay curves are shown in the inset of Fig. 9(c) along with exponential curves fitted to these data. The half-life was taken from the average of value of both 87 keV and 348 keV transitions in both the clover and planar detectors. According to the Weisskopf estimates, a 348 keV $M2$ γ-ray transition would have a 288 ns half-life, which is reduced to 180 ns when internal conversion is considered. A 348 keV γ-ray transition with multipolarities $M1$ or $E2$ would have half-lives of 0.16 ps and 2.7 ns, respectively. The possibility of the 87 keV transition being a transition with a high multipolarity is ruled out as this would yield a half-life far greater than the measured 700(10) ns. A 87 keV $M1$ transition has a Weisskopf estimate of 27.1ps, therefore the 348 keV $M2$ transition is assigned to directly depopulate the isomeric state. Combining the intensity flow, half-life, and internal conversion measurements, the multipolarities for the 348 keV and 87 keV transitions are $M2$ and $M1$, respectively. Assuming the 87 keV transition feeds the $7/2^-$ ground state, then the isomer must have $I^\pi = 13/2^+$, considering a spin change of three units and a change in parity. The excitation energy of the isomeric state is 434.3(4) keV, given by sum of the two γ-ray transition energies.

Previously, in-beam γ-ray spectroscopy has been performed for ^{167}Os [12], from which the yrast band bandhead

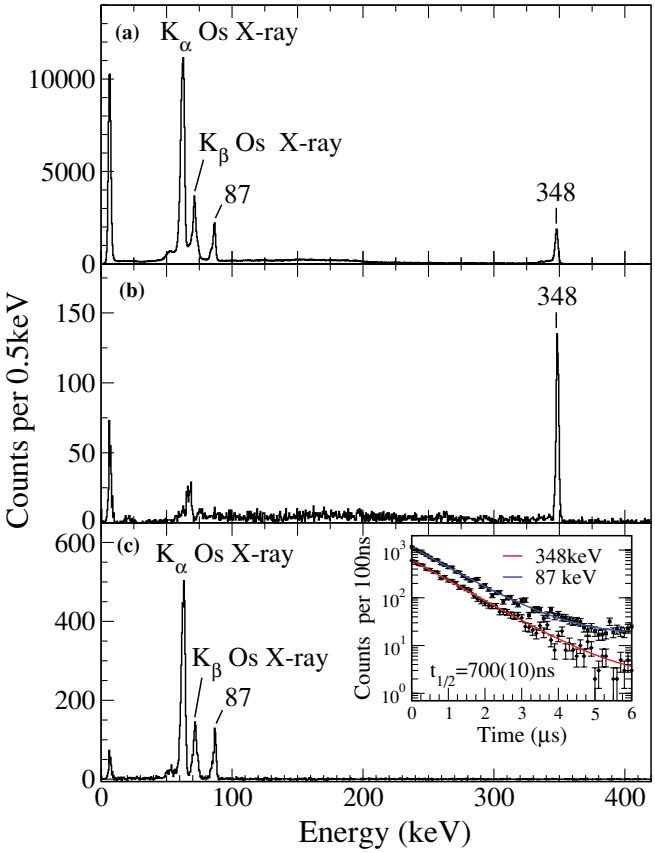

FIG. 9. (Color online) (a) An energy spectrum of γ-ray transitions measured in the clover and planar detectors within 3 μs of a recoil implant in the DSSDs, correlated with the α decay of ^{167}Os within a maximum correlation time of 3 s. These data were taken from the total run time of reaction 3 and 4. (b) A spectrum of γ rays measured in the clover detector in coincidence with the 87 keV transition measured in the planar detector. (c) A spectrum of γ rays measured in the planar detector in coincidence with the 348 keV transition measured in the clover detector. The inset in (c) shows time differences between the 87 keV transition in the planar detector and a recoil in the DSSD and the 348 keV transition in the clover detector and a recoil in the DSSD. The recoil implant is tagged with the α decay of ^{167}Os. An exponential fit of the form $N = N_0e^{-\lambda t} + N_1e^{-\lambda 1t}$, is shown by the solid/red and blue lines. The spectra shown in (b) and (c) are taken from reaction 4 only.

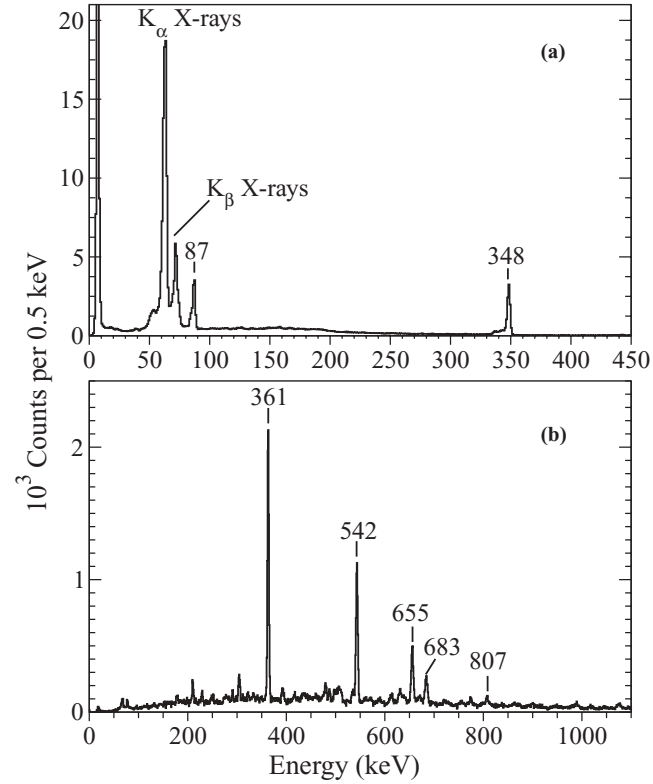

FIG. 10. (a) Spectrum showing the energies of γ-ray transitions detected in the GREAT planar and clover detectors within 3 μs of a recoil implantation in the DSSDs and correlated with the yrast band [marked transitions in (b)] of ^{167}Os detected in JUROGAM up to 2 μs before a recoil implant. (b) Spectrum showing γ rays detected in JUROGAM in delayed coincidence with the 87 keV and 348 keV γ rays detected in the GREAT planar and clover detectors. Each spectrum contains the summed data from experiments 3 and 4.

was predicted to be $I^\pi = 13/2^+$, based on an $i_{13/2}$ neutron decoupled from the core. This assignment was based on the energy level systematics of Os isotopes, but the excitation energy of this state was not given. In order to verify that the isomeric state is fed by the yrast sequence, RIT was performed. The 87 keV and 348 keV transitions are shown, in Fig. 10(a), to be in delayed coincidence with the known γ-ray transitions from the yrast sequence above the $13/2^+$ state. Consequently, Fig. 10(b) shows that yrast band of ^{167}Os can be unambiguously identified using the 87 keV and 348 keV transitions as a 'tag.'

Therefore, whether taking a bottom up approach from the ground state or a top down approach from the $I^\pi = 13/2^+$ bandhead, which has been shown to be the observed isomeric state, the same result is achieved. A partial level scheme for ^{167}Os is shown in Fig. 11.

C. $^{171}_{74}$Pt$_{93}$

Nuclei of ^{171}Pt were produced in reaction 5, detailed in Table I. A total of 1.0×10^6 recoil-correlated ^{171}Pt α decays were collected during the experiment within a maximum correlation time of 150 ms, the spectrum of which is shown in Fig. 12(a). The α-decay half-life was measured to be $t_{1/2} = 48(1)$ ms. The decay curve of ^{171}Pt and a fit to the data using the prescription of Schmidt [33] is shown in Fig. 12(b). The ^{171}Pt α-particle energy of 6453(3) keV [40] was used as one of the calibration points, therefore no improvement was made for this value.

A total of 2.3×10^5 focal-plane γ rays were correlated with the α decay of ^{171}Pt, within 4 μs of a recoil implant. Figure 13 shows the planar plus clover (^{171}Pt)α-tagged γ-ray spectrum, where γ-ray photopeaks at 89.5(7) keV and 323.1(6) keV, along with Pt X-rays are clearly visible.

From a set of a asymmetric two-dimensional matrices, γ-γ and CE-γ ray coincidences [shown in Fig. 14(a)–14(c)] confirm that these two transitions are in coincidence.

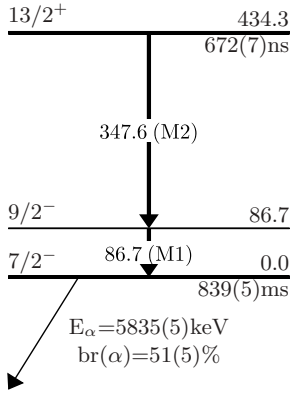

FIG. 11. A partial level scheme of ^{167}Os showing the decay path from the $13/2^+$ isomeric state and the ground-state α-decay information. The α-decay energy is taken from Ref. [4].

The α_K values were extracted from the ratio of K X-rays to γ rays for both the 90 keV and 323 keV transitions. The α_K values were measured to be 7.5(10) and 0.65(12) for the 90 keV and 323 keV transitions, respectively. The theoretical α_K values for a 90 keV $M1$, $E1$, and $E2$ transition are 7.4, 0.42, and 0.76 [36], respectively. Therefore, the 90 keV transition is assigned an $M1$ multipolarity. Only the theoretical α_K value of 0.71(1) for a 323 keV $M2$ transition is consistent with the experimental value of 0.65(12). In addition, the α_K/α_{LM} ratio was measured to be 3.5(5) for the 323 keV transition (see Fig. 14). This is consistent with the theoretical value of $\alpha_K/\alpha_{LM} = 3.6$ for an $M2$ transition [36]. The 323 keV transition is therefore assigned an $M2$ multipolarity. These findings are summarized in Table II.

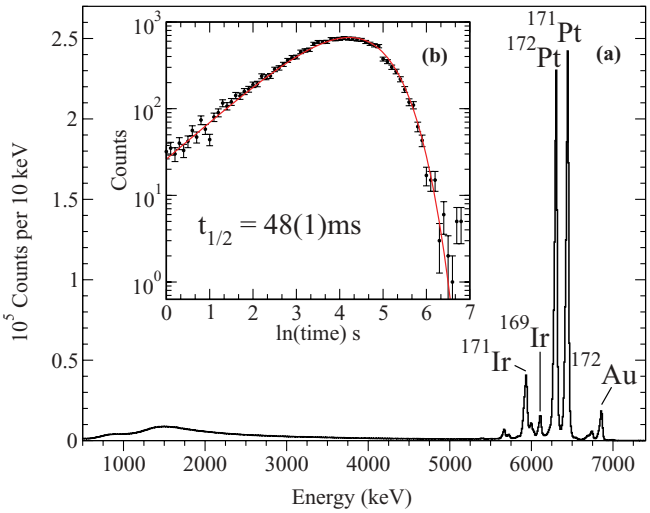

FIG. 12. (Color online) (a) A spectrum taken from reaction 5 of α-decay energies correlated with a recoil implant in the DSSDs within a maximum search time of 150 ms. (b) The time differences between a recoil implant and the α decay of ^{171}Pt, correlated within 960 ms of a recoil, also correlated to the daughter decay ^{167}Os and granddaughter decay ^{163}W, within correlation times of 2.73 s and 8 s, respectively. The fit to the data was produced using Eq. (8) in Ref. [33] and is shown in by the solid/red line.

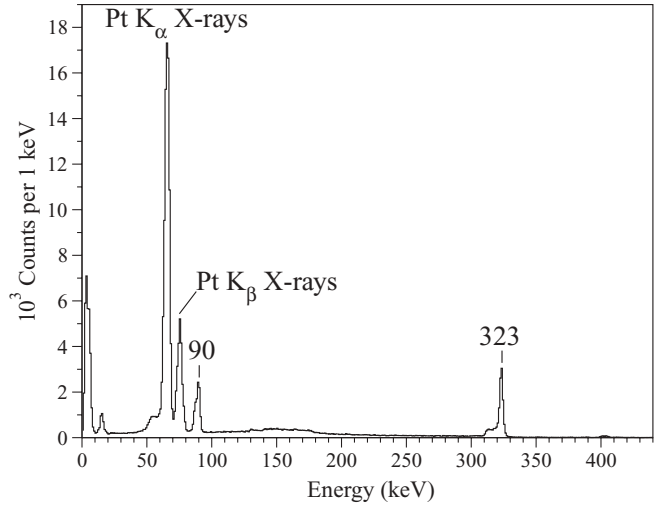

FIG. 13. A spectrum showing γ-ray energies from the clover and planar detectors, correlated with the α decay of ^{171}Pt. The γ rays were collected within 4 μs of a recoil implant in the DSSDs.

The half-life of the isomeric state was measured to be $t_{1/2} = 901(9)$ ns, from the time difference between recoils in the DSSDs and both γ-ray transitions in the clover and planar detectors and conversion electrons in the PIN diodes. A sample decay curve is shown in the inset of Fig. 14(b). This half-life is within the single-particle transition rate range for a hindered 323 keV $M2$ transition. Any other transition multipolarity is more than two orders of magnitude away in terms of half-life. The Weisskopf estimate for any multipolarity 90 keV transition does not fit the measured half-life. The nearest half-life estimate is 1.67 μs for an $E2$ transition, but this is ruled out on the basis of the measured α_K value. The Weisskopf estimate for a 90 keV $M1$ transition is 24.5 ps, therefore the 323 keV transition is assigned to feed directly from the isomer. The intensity flow for these transitions is also consistent with these finding and are tabulated in Table II.

Previous RDT studies of ^{171}Pt have reported excited states built on the $13/2^+$ state [13–15]. Cederwall *et al.* [14] first reported excited states in ^{171}Pt. Comparing the experimental results to TRS plus QRPA calculations they deduced that the observed band was based on an $i_{13/2}$ neutron decoupled from the core and that this nucleus has a collective-vibrational character. The excitation energy of the $13/2^+$ state was not discussed. Seweryniak *et al.* [13] drew similar conclusions to Cederwall *et al.* [14], due to the striking similarity between the states observed and the ground-state band of ^{172}Pt, but again the excitation of the bandhead was not mentioned. Bäck *et al.* [15] suggested that the ground state was built on an $i_{13/2}$ neutron configuration based on the positive parity minimum lying slightly lower than the negative parity minimum from TRS calculations. To confirm the isomeric state is fed by the previously observed yrast structure of ^{171}Pt, RIT was performed. Both conversion electrons and γ rays from the focal plane of RITU were correlated with prompt γ-ray transitions in the JUROGAM array. The resulting spectra are shown in Fig. 15 and confirm that transitions observed at the focal

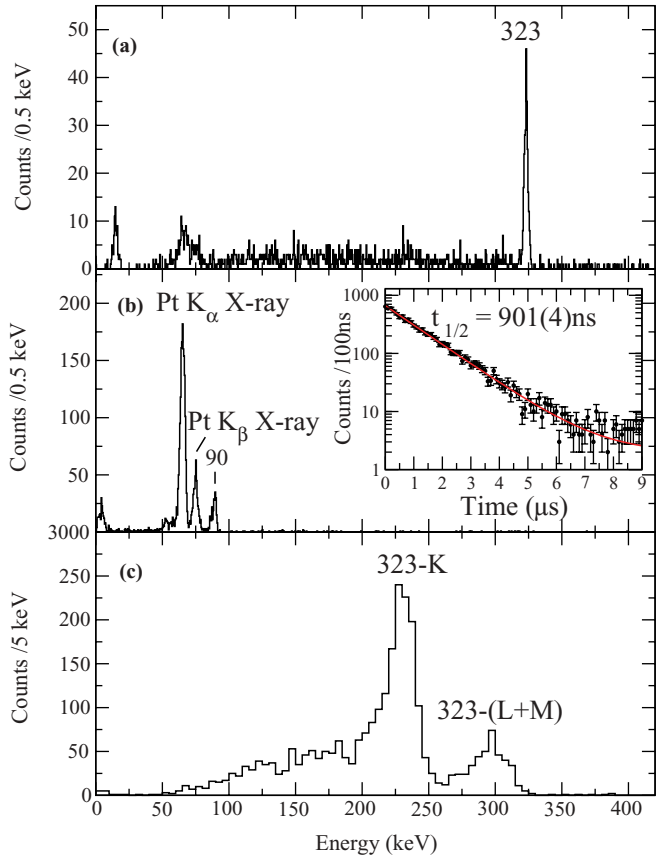

FIG. 14. (Color online) (a) An energy spectrum of γ-ray transitions in the clover detector in coincidence with the 90 keV transition in the planar detector. (b) A spectrum of γ-ray energies in the planar detector in coincidence with the 323 keV γ-ray in the clover detector. (c) An energy spectrum of conversion electrons in the PIN-diodes gated by the 90 keV γ-ray transition in both the clover and planar detectors. A 4 μs time gate between either a γ ray or conversion electron and a recoil is applied to all spectra. The inset of (b) shows the decay curve of the 90 keV γ ray and the (red) line is an exponential fit to these data. These data are taken from reaction 5 are associated to ^{171}Pt.

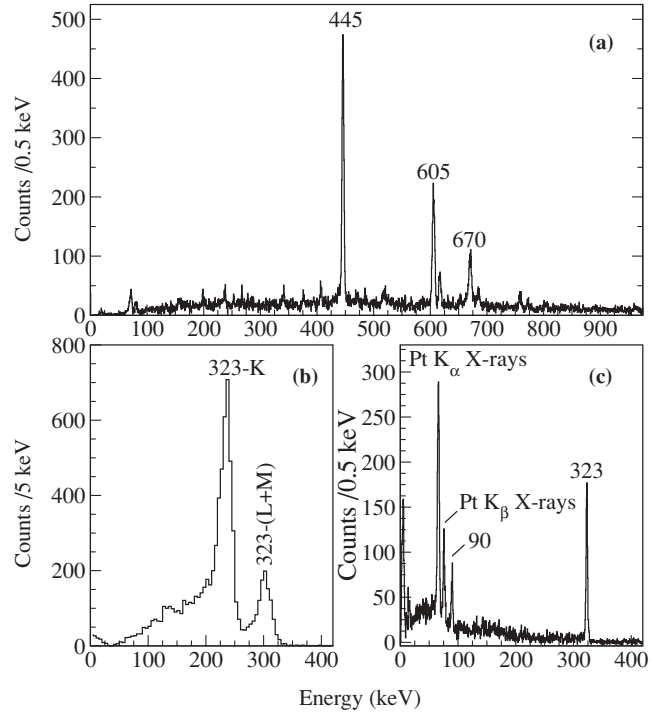

FIG. 15. (a) A γ-ray energy spectrum recorded in JUROGAM produced by gating on the 90 keV and 323 keV transitions in the clover and planar detectors, plus the 323-L and 323-K conversion electrons in the PIN-diodes. (b) A conversion electron spectrum produced by gating on the prompt γ-ray transitions in JUROGAM with energies of 445 keV, 605 keV, and 740 keV. (c) A delayed γ-ray spectrum from the clover plus planar detectors with the same gates as (b). All focal plane γ rays and conversion electron's were collected within 4 μs of a recoil implant in the DSSDs. These data are taken from reaction 5 and shows transitions associated to ^{171}Pt.

plane are in delayed coincidence with previously observed prompt transitions built on the $13/2^+$ state [13–15]. This eliminates the possibility of the ground state being a $\nu i_{13/2}$ configuration.

A partial level scheme for ^{171}Pt is shown in Fig. 16. Again, whether a bottom up approach is taken from the $I^\pi = 7/2^-$ ground state or a top down approach is taken from the $I^\pi = 13/2^+$ bandhead the result is the same; the 323 keV $M2$ transition depopulates the isomeric state, therefore the state it populates has $I^\pi = 9/2^-$ and in turn the 90 keV $M1$ transition then populates the $I^\pi = 7/2^-$ ground state.

IV. DISCUSSION

Traditionally, systematic trends of nuclei are presented in terms of isotonic or isotopic chains, thus fixing either the proton or neutron number. In the case of α-decay chains both neutron and proton numbers vary and the only constant is the number of valence nucleons outside of closed shells. For even-N and even-Z nuclei one may turn to the IBM models in order to explain these nuclei. In the case of odd-A nuclei the picture is not so clear, but in an ad hoc

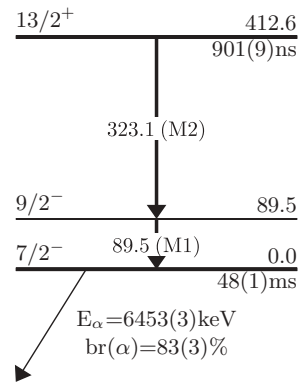

FIG. 16. A partial level scheme of ^{171}Pt showing the decay path from the $13/2^+$ isomeric state and the ground-state α-decay information. The α-decay energy is taken from Ref. [40].

manner one can use the F-spin concept in order to compare these nuclei. F-spin in the boson system is analogous to isospin in the fermion system [41] (and references therein). Neutron bosons have $F = \frac{1}{2}$ and $F_0 = -\frac{1}{2}$, whereas proton bosons have $F = \frac{1}{2}$ and $F_0 = +\frac{1}{2}$. Consequently, the total F-spin of a nucleus can range from $F_{\min} = |N_\nu - N_\pi|$ to $F_{\max} = N_\nu + N_\pi$, where $N_{\pi,\nu}$ is the number of proton(π) and neutron(ν) bosons, respectively. The total F_0 of a nucleus is given by $F_0 = \frac{1}{2}(N_\pi - N_\nu)$. Hence, series of F-spin multiplets are formed across major shells, which have the same F-spin yet differ by F_0. In Fig. 17 the systematics of the three lowest-lying states of the F-spin multiplet $F_{\max} = 7.5$ are plotted as a function of Z for nuclei between $N = 82$ and $Z = 82$. The similarities between these nuclei is most apparent. In all cases, the ground state has $I^\pi = 7/2^-$ and the lowest excited state is $I^\pi = 9/2^-$ with a $I^\pi = 13/2^+$ state lying a few hundred keV higher in excitation energy. It is thought that these states originate from the $\nu f_{7/2}$, $\nu h_{9/2}$, and $\nu i_{13/2}$ orbitals, respectively, thus the single-quasiparticle energy differences between the $\nu f_{7/2}$, $\nu h_{9/2}$, and $\nu i_{13/2}$ states are reflected in Fig. 17. As can be seen the energy differences between the $13/2^+$ and $9/2^-$ states remains almost constant across this decay chain down to $N = 85$. This is quite remarkable as at $N = 83$, the $13/2^+$ state in ^{151}Er is no longer a pure $\nu i_{31/2}$ state, but has been explained as a combination of an $i_{13/2}$ neutron with an admixture of $\nu f_{7/2} \otimes 3^-$, which is formed from an octupole excitation of the core [32]. This scenario is not expected in the heavier isotopes of this chain as the octupole states in the core nuclei are at excitation energies of 1.51 MeV for ^{166}Os [42] and 1.56 MeV for ^{170}Pt [43]. Contrary to the $\nu i_{13/2} - \nu h_{9/2}$ energy differences, the energy difference between the $\nu f_{7/2}$ and $\nu h_{9/2}$ states changes as $N = 82$ is approached, but not as $Z = 82$ is approached. This indicates that the states near the neutron Fermi surface are, not surprisingly, more affected by the neutron, rather than the proton closed shell. In the study of isotonic chains it has been observed that as the $\pi h_{11/2}$ shell is filled the $\nu h_{9/2}$ drops in energy due to the spin-orbit partner attraction. From $N = 83$ to $N = 89$ there is a pronounced lowering of the $h_{9/2}$ state with respect to the ground state, but this effect appears to saturate at $Z = 74$, which interestingly is the midpoint between $N = 82$ and $Z = 82$, hence F_0 is at a minimum and $N_\pi N_\nu$ is at a maximum. Also, when moving from $N = 83$ to $N = 93$ one may expect that the ground-state configuration would change as the $\nu f_{7/2}$ orbital is filled and the $\nu h_{9/2}$ is opened. As can be seen from these studies, this is not the case. Thus the almost constant energy difference between these three low-lying single-quasiparticle states, must somehow be strongly related to the only constant; the valence particle number. As either the $N = 82$ or $Z = 82$ shell closures are approached a drop in deformation is expected. Traversing the α-decay chain from ^{175}Hg to ^{151}Er is a transition that moves away from the $Z = 82$ shell closure and at the same time moves toward the $N = 82$ shell closure, hence the change in deformation is minimized.

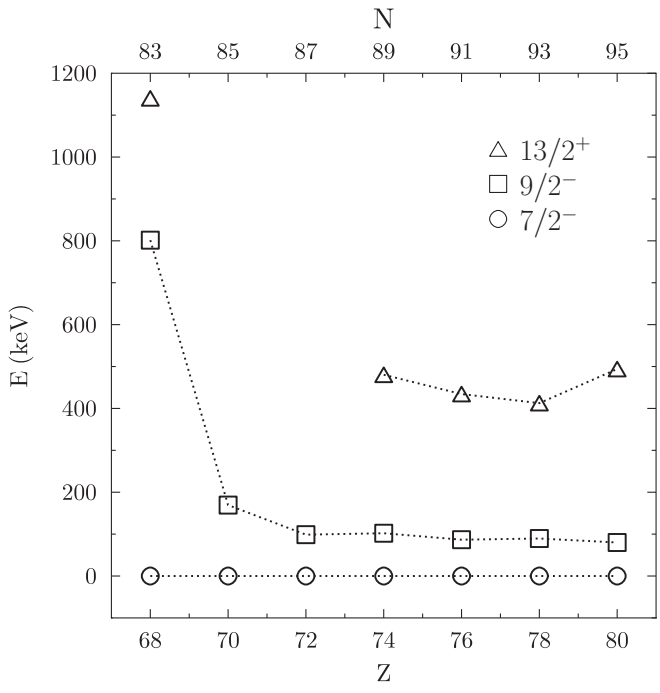

FIG. 17. A plot of the excitation energies of the $9/2^-$ state and $13/2^+$ state relative to the $7/2^-$ ground state for even-Z odd-N isotopes with $F_{\max} = 7.5$. Values for $^{151}_{68}\mathrm{Er}_{83}$, $^{155}_{70}\mathrm{Yb}_{85}$, and $^{159}_{72}\mathrm{Hf}_{87}$ are taken from Refs. [30–32], respectively, $^{163}_{74}\mathrm{W}_{89}$, $^{167}_{76}\mathrm{Os}_{91}$, and $^{171}_{78}\mathrm{Pt}_{93}$ are from this work and $^{175}_{80}\mathrm{Hg}_{95}$ is taken from [7].

The $B(M2)$ values are given by

$$B(M2) = \frac{3.12 \times 10^7}{A^{2/3} E_\gamma^5 t_{1/2}(1 + \alpha_{tot})/br\%}\,\mathrm{W.u.}, \qquad (1)$$

where E_γ is in keV and $t_{1/2}$ is in seconds. For ^{171}Pt, ^{167}Os, and ^{163}W the $B(M2)$ values have been deduced for the $M2$ transitions depopulating the isomeric states and are 0.19(2) W.u., 0.19(4) W.u., and 0.18(4) W.u., respectively. The $B(M2)$ values are constant within errors. The transitions are between the $13/2^+$ and $9/2^-$ states and should be single particle in nature, representing a change from an $i_{13/2}$ neutron state to an $h_{9/2}$ neutron state. A hindrance of $\approx$5 is observed for the $M2$ transitions as exhibited in the small $B(M2)$ values for these transitions. Retarded $M2$ transitions have been observed across the nuclear chart, the reasons for which vary from its spin-flip character, core polarization, exchange currents reducing the spin magnetism, impure initial and/or final states, to a change in shape [32,44–48]. It is possible that all these factors are at work. It is suffice to say that the majority of $M2$ transitions are retarded to a degree ranging from 1 to 1000 and that further discussion of this point is beyond the scope of this paper.

The $B(M2, \nu i_{13/2} \rightarrow \nu h_{9/2})$ values have previously been measured for ^{151}Er [32] and ^{175}Hg [7] and are 0.24 and 0.16(1), respectively. Though part of the systematics are missing, the $B(M2, \nu i_{13/2} \rightarrow \nu h_{9/2})$ values remain almost constant within errors between the $Z = 80$ down the α-decay chain of ^{175}Hg to $N = 83$.

In ^{163}W another state with spin and parity $11/2^-$ is observed. The lack of an $M1$ transition between the $11/2^-$ and $9/2^-$ states indicates a large hindrance of any transition between these states and emphasises the strength of the $E2$ transition between the $11/2^-$ and $7/2^-$ states. It is therefore

assigned to be the lowest transition in the ground-state rotational band. This result has been confirmed by Joss *et al.* [49] using the data taken from reaction 1. Similar transitions are not seen in ^{171}Pt or ^{167}Os, which indicates that the first $11/2^-$ state is either at a comparable or higher energy than the $13/2^+$ state.

V. SUMMARY

In summary, the decays of the isomeric $13/2^+$ band head to the ground state in ^{171}Pt, ^{167}Os, and ^{163}W have been observed for the first time. Alpha-decay hindrance factors show that all three nuclei have the same spin and parity ground state. In addition, conversion electron and γ-ray spectroscopy have confirmed the assignment of the ground-state spin and parity of $I^\pi = 7/2^-$ to these nuclei for the first time. The decay sequence between the $I^\pi = 13/2^+$ isomers and the $I^\pi = 7/2^-$ ground state show the single-quasiparticle energy differences between the $\nu f_{7/2}$, $\nu h_{9/2}$, and $i_{13/2}$ states across the α-decay chain of ^{171}Pt, ^{167}Os, and ^{163}W.

ACKNOWLEDGMENTS

This work has been supported by the Academy of Finland under the Finnish Centre of Excellence Programme (Project Nos. 44875 and 213503), the Swedish Research Council, the Göran Gustafsson Foundation, the EU FP5(HPRI-CT-1999-00044) and EXOTAG (HPRI-1999-CT-50017), through the EU-FP6-I3 project EURONS (RII3-CT-2004-506065), and the UK Engineering and Physical Sciences Research Council and Science and Technology Facilities Council. C.S. (209430), P.N. (121110), and P.T.G. (111965) acknowledge the support of the Academy of Finland; V.M., M.S., and I.G.D. acknowledge support from the EC Marie Curie Actions grant; V.M. acknowledges the Slovak Research and Development Agency (Contract No. APVV-20-006205); and E.I. and M.N. support from the JSPS Core-to-Core Program, International Research Network for Exotic Femto Systems. We thank the UK/France (STFC/IN2P3) Loan Pool and GAMMAPOOL European Spectroscopy Resource for the loan of the detectors for JUROGAM and GSI for the loan of the VEGA (1/4018/07) detectors.

[1] A. N. Andreyev, M. Huyse, P. Van Duppen, J. F. C. Cocks, K. Helariutta, H. Kettunen, P. Kuusiniemi, M. Leino, W. H. Trzaska, K. Eskola *et al.*, Phys. Rev. Lett. **82**, 1819 (1999).

[2] A. N. Andreyev, K. Van de Vel, A. Barzakh, A. De Smet, H. De Witte, D. V. Fedorov, V. N. Fedoseyev, S. Franchoo, M. Gorska, M. Huyse *et al.*, Eur. Phys. J. A **14**, 63 (2002).

[3] D. G. Jenkins, A. N. Andreyev, R. D. Page, M. P. Carpenter, R. V. F. Janssens, C. J. Lister, F. G. Kondev, T. Enqvist, P. T. Greenlees, P. M. Jones *et al.*, Phys. Rev. C **66**, 011301(R) (2002).

[4] R. D. Page, P. J. Woods, R. A. Cunningham, T. Davinson, N. J. Davis, A. N. James, K. Livingston, P. J. Sellin, and A. C. Shotter, Phys. Rev. C **53**, 660 (1996).

[5] C. R. Bingham, K. S. Toth, J. C. Batchelder, D. J. Blumenthal, L. T. Brown, B. C. Busse, L. F. Conticchio, C. N. Davids, T. Davinson, D. J. Henderson *et al.*, Phys. Rev. C **54**, R20 (1996).

[6] A. Melerangi, D. Appelbe, R. D. Page, H. J. Boardman, P. T. Greenlees, P. Jones, D. T. Joss, R. Julin, S. Juutinen, H. Kettunen *et al.*, Phys. Rev. C **68**, 041301(R) (2003).

[7] D. O'Donnell, J. Simpson, C. Scholey, T. Bäck, P. Greenlees, U. Jakobsson, P. Jones, D. Joss, D. Judson, R. Julin *et al.*, Phys. Rev. C **79**, 051304(R) (2009).

[8] K. H. Schmidt, R. S. Simon, J. G. Keller, F. P. Hessberger, G. Munzenberg, B. Quint, H. G. Clerc, W. Schwab, U. Gollerthan, and C. C. Sahm, Phys. Lett. **B168**, 39 (1986).

[9] E. S. Paul, P. J. Woods, T. Davinson, R. D. Page, P. J. Sellin, C. W. Beausang, R. M. Clark, R. A. Cunningham, S. A. Forbes, D. B. Fossan *et al.*, Phys. Rev. C **51**, 78 (1995).

[10] D. M. Cullen, N. Amzal, A. J. Boston, P. A. Butler, A. Keenan, E. S. Paul, H. C. Scraggs, A. M. Bruce, C. M. Parry, J. F. C. Cocks *et al.*, Phys. Rev. C **58**, 846 (1998).

[11] C. Scholey, D. M. Cullen, E. S. Paul, A. J. Boston, P. A. Butler, T. Enqvist, C. Fox, H. C. Scraggs, S. L. Shepherd, O. Stezowski *et al.*, Phys. Rev. C **63**, 034321 (2001).

[12] D. T. Joss, S. L. King, R. D. Page, J. Simpson, A. Keenan, N. Amzal, T. Back, M. A. Bentley, B. Cederwall, J. F. C. Cocks *et al.*, Nucl. Phys. **A689**, 631 (2001).

[13] D. Seweryniak, D. Ackermann, H. Amro, L. T. Brown, M. P. Carpenter, L. Conticchio, C. N. Davids, S. M. Fischer, G. Hackman, S. Hamada *et al.*, Phys. Rev. C **58**, 2710 (1998).

[14] B. Cederwall, T. Bäck, R. Bark, S. Tormanen, S. Odegard, S. L. King, J. Simpson, R. D. Page, N. Amzal, D. M. Cullen *et al.*, Phys. Lett. **B443**, 69 (1998).

[15] T. Bäck, B. Cederwall, K. Lagergren, R. Wyss, A. Johnson, P. Greenlees, D. Jenkins, P. Jones, D. T. Joss, R. Julin *et al.*, Eur. Phys. J. A **17**, 1 (2003).

[16] G. D. Dracoulis, B. Fabricius, P. M. Davidson, A. O. Macchiavelli, J. Oliveira, J. Burde, F. Stephens, and M. A. Deleplanque, Contributions to the International Conference on Nuclear Structure at High Angular Momentum (1992).

[17] G. Dracoulis (private communication, 2007).

[18] G. Audi, O. Bersillon, J. Blachot, and A. H. Wapstra, Nucl. Phys. **A729**, 3 (2003).

[19] P. Moller, J. R. Nix, and K. L. Kratz, At. Data Nucl. Data Tables **66**, 131 (1997).

[20] M. Leino, J. Äystö, T. Enqvist, P. Heikkinen, A. Jokinen, M. Nurmia, A. Ostrowski, W. H. Trzaska, J. Uusitalo, K. Eskola *et al.*, Nucl. Instrum. Methods Phys. Res. B **99**, 653 (1995).

[21] P. T. Greenlees, A. N. Andreyev, J. Bastin, F. Becker, E. Bouchez, P. A. Butler, J. F. C. Cocks, Y. Le Coz, K. Eskola, J. Gerl *et al.*, Eur. Phys. J. A **20**, 87 (2004).

[22] C. W. Beausang, S. A. Forbes, P. Fallon, P. J. Nolan, P. J. Twin, J. N. Mo, J. C. Lisle, M. A. Bentley, J. Simpson, F. A. Beck *et al.*, Nucl. Instrum. Methods Phys. Res. A **313**, 37 (1992).

[23] C. R. Alvarez, Nucl. Phys. News **3**(3), 10 (1993).

[24] R. D. Page, A. N. Andreyev, D. E. Appelbe, P. A. Butler, S. J. Freeman, P. T. Greenlees, R. D. Herzberg, D. G. Jenkins, G. D. Jones, P. Jones *et al.*, Nucl. Instrum. Methods Phys. Res. B **204**, 634 (2003).

[25] A. N. Andreyev, P. A. Butler, R. D. Page, D. E. Appelbe, G. D. Jones, D. T. Joss, R. D. Herzberg, P. H. Regan, J. Simpson, and R. Wadsworth, Nucl. Instrum. Methods Phys. Res. A **533**, 422 (2004).

[26] I. H. Lazarus, D. E. Appelbe, P. A. Butler, P. J. Coleman-Smith, J. R. Cresswell, S. J. Freeman, R. D. Herzberg, I. Hibbert, D. T. Joss, S. C. Letts *et al.*, IEEE Trans. Nucl. Sci. **48**, 567 (2001).
[27] P. Rahkila, Nucl. Instrum. Methods Phys. Res A **595**, 637 (2008).
[28] W. T. Milner, UPAK, The Oak Ridge Analysis Package, Oak Ridge National Laboratory, Oak, Ridge, Tennessee 37831 (private communication).
[29] J. O. Rasmussen, Phys. Rev. **113**, 1593 (1959).
[30] K. Y. Ding, J. A. Cizewski, D. Seweryniak, H. Amro, M. P. Carpenter, C. N. Davids, N. Fotiades, R. V. F. Janssens, T. Lauritsen, C. J. Lister *et al.*, Phys. Rev. C **62**, 034316 (2000).
[31] K. Y. Ding, J. A. Cizewski, D. Seweryniak, H. Amro, M. P. Carpenter, C. N. Davids, N. Fotiades, R. V. F. Janssens, T. Lauritsen, C. J. Lister *et al.*, Phys. Rev. C **64**, 034315 (2001).
[32] R. Barden, A. Plochocki, D. Schardt, B. Rubio, M. Ogawa, P. Kleinheinz, R. Kirchner, O. Klepper, and J. Blomqvist, Z. Phys. A **329**, 11 (1988).
[33] K. H. Schmidt, C. C. Sahm, K. Pielenz, and H. G. Clerc, Z. Phys. A **316**, 19 (1984).
[34] S. Hofmann, W. Faust, G. Munzenberg, W. Reisdorf, P. Armbruster, K. Guttner, and H. Ewald, Z. Phys. A **291**, 53 (1979).
[35] D. A. Eastham and I. S. Grant, Nucl. Phys. **A208**, 119 (1973).
[36] T. Kibedi, T. W. Burrows, M. B. Trzhaskovskaya, P. M. Davidson, and C. W. Nestor, Nucl. Instrum. Methods Phys. Res. A **589**, 202 (2008).
[37] T. Lonnroth, Z. Phys. A **331**, 11 (1988).
[38] S. Hofmann, G. Munzenberg, F. Hessberger, W. Reisdorf, P. Armbruster, and B. Thuma, Z. Phys. A **299**, 281 (1981).
[39] H. A. Enge, M. Salomaa, A. Sperduto, J. Ball, W. Schier, A. Graue, and A. Graue, Phys. Rev. C **25**, 1830 (1982).
[40] A. Rytz, At. Data Nucl. Data Tables **47**, 205 (1991).
[41] B. R. Barrett, G. D. Dracoulis, and R. A. Bark, Phys. Rev. C **43**, R926 (1991).
[42] D. E. Appelbe, J. Simpson, M. Muikku, H. J. Boardman, A. Melarangi, R. D. Page, P. T. Greenlees, P. M. Jones, R. Julin, S. Juutinen *et al.*, Phys. Rev. C **66**, 014309 (2002).
[43] D. T. Joss, J. Simpson, D. E. Appelbe, C. J. Barton, D. D. Warner, K. Lagergren, B. Cederwall, B. Hadinia, S. Eeckhaudt, T. Grahn *et al.*, Phys. Rev. C **74**, 014302 (2006).
[44] D. Kurath and R. D. Lawson, Phys. Rev. **161**, 915 (1967).
[45] J. Keinonen, R. Rascher, M. Uhrmacher, N. Wust, and K. P. Lieb, Phys. Rev. C **14**, 160 (1976).
[46] H. Ejiri, T. Shibata, and M. Fujiwara, Phys. Rev. C **8**, 1892 (1973).
[47] T. Lönnroth, C. W. Beausang, D. B. Fossan, L. Hildingsson, W. F. Piel, M. A. Quader, S. Vajda, T. Chapuran, and E. K. Warburton, Phys. Rev. C **33**, 1641 (1986).
[48] P. Nieminen, S. Juutinen, A. N. Andreyev, J. F. C. Cocks, O. Dorvaux, K. Eskola, P. T. Greenlees, K. Hauschild, K. Helariutta, M. Huyse *et al.*, Phys. Rev. C **69**, 064326 (2004).
[49] D. T. Joss, J. Thomson, C. Scholey, S. Erturk, J. Simpson, R. D. Page, L. Bianco, B. Cederwall, I. G. Darby, S. Eeckhaudt *et al.*, Proceedings of Nuclear Physics and Astrophysics: From Stable Beams to Exotic Nuclei (2008).